Stability of FG material micro-pipe conveying fluid

Talib EH. Elaikh, Nada M. Abed

Department of Mechanical Engineering, College of Engineering, Thi-Qar University, Iraq.

Abstract
Functionally gradient materials and small-scale pipes have great importance in the industry because of its wide applications in many engineering fields such as fluid transport in fluidic devices. In this article, an analytical solution for the stability of functionally graded (FG) material micro-pipe fluid-conveying is offered. The properties of the material are changed constantly across the micro-pipes thickness and depend on power law distribution. Hamilton's principle, Euler beam model, and modified coupled stress theory are utilized to get an equation of motion for conservative FG micro-pipe (Simply supported and clamped-clamped). The vibration equation of FG micro-pipe is converted from 4th order to a 2nd order using the Galerkin's method. Solving the Eigenvalue problem results in a distinct equation depicting the frequency relationship of the parameters. By plotting the root locus of the characteristic equations, the main stability characteristics such as stability, instability, and flutter are studied graphically. The effect of different parameters such as gradient index, length scale, fluid velocity, micro flow parameter, and mass ratio on FG micro-pipe was studied. The results showed that each parameter had a significant impact on the behavior of stability as the chain of stability could change significantly.

1. Introduction
Pipes convey fluid have wide applications in engineering and industrial fields. More recently, this topic has been developed in the study and analysis of Fluid-Structure Interaction (FSI) which has great applications in aerodynamics, aerospace, medical engineering, ship movement, etc. Pipes fluid-conveying are classified as gyroscopic system according to a gyroscopic effect due to the relative rotational movement of the fluid element, which vibrates sideways to adapt to the movement of the tubes. In general, pipe fluid-conveying systems operate at a relatively low (pre-critical) velocity. At some critical speeds, the pipes may lose their stability either by oscillating the growth of the ace (flutter) or by the static convergence (buckle). When more high-velocity (post-critical) pipes are made in a different way, they can still stabilize in the same position (flutter or buckle), restore stability or change their instability.

The assessment of the stability zones at the parameters of the different pipes is important in the design of such systems to ensure the desirability of safe operation of specific parameters for liquids and pipes. Simply support, clamped and clamped-pinned pipes belong to this category. Several researchers have analyzed and studied their persistence in the pipe fluid-conveying such as Weaver and Unny [1], Bishop et al [2] and Si-Ung et al [3]. Their investigations focused on assessing the critical fluid velocity of instability and stability properties for simply supported, clamped and clamped-pinned pipes.

In addition, these investigations were based on a complete solution of vibration equation using numerical or analytical solutions. Huseyni and Plaut [4] and Huseyni [5] expanded the stability analysis to include flutter instability in non-conservative systems such as clamped-free with the distribution of follower load. They have shown that flutter instability can occur in such systems and buckling instabilities. Kuiper and Metrlkine [6] studied the buckling stability for the gyroscopic conservative beams that subjected to a follower load. Several useful theories have been introduced on the impact of gyroscopic power disparities on areas of instability and buckling stability. Li-Qun [7] has recently analyzed the instability of the axially moving beam with simply support or clamped-clamped ends condition. A reserved quantity has been applied to explain the stability of the linear equilibrium configuration in the transverse lines of the low-speed coaxial beam.

Flutter and buckling instability for a conservative and non-conservative beam was investigated by Elfelsou [8]. Buckling loads and the natural frequencies were found for conservative beam while a flutter load and an instability region were specified for the non-conservative beams. One mode analysis was used to analyze an Eigen-modes and nonlinear vibration.

The similarities between the dynamics of fluid-conveying pipes and other dynamic problems such as columns under follower loads, the moving strings and belts, and the beams with moving loads have been explained by many researchers such as Plaut [9] who have shown that dynamic behavior of pipe systems is similar to follower loads beams. Recently, Païdoussis [10] published the idea of analogy between piping systems and other dynamic systems, also, the possibility of sharing knowledge gained between each other. Yusuf et al. [11] analyzed fluid stability in fluid transfer using the Galerkin's method. The results showed that the mass ratio has an effect on the stability behavior as its stability can change significantly, while liquid pressure showed little effect because the stability sequence does not change for a large range of fluid velocities. Jweeg and Ntayeesh [12] studied the critical buckling velocities for conservative pipes fluid-conveying rested on different end conditions experimentally. A semi-analytic solution was used to find the frequency and critical velocity for (clamped-clamped, simply support, and clamped-pinned pipes) end conditions. The new an experimental approach for estimating the buckling critical velocities of measuring various natural frequencies at relatively small-flow rates were offered.

Through the literature mentioned above, it was found that the articles available for studying the stability of FGM micro-pipe very little. The stability boundary of conservative FG micro pipes fluid conveying is investigated in this paper. To perform this analysis the vibration equation is discretized to second-degree of freedom by employing Galerkin's method. The various boundaries of the stable and unstable regions can simply be investigated by studying the influence of the gradient index, fluid velocity, micro flow parameter, mass ratio, length scale on the stability of FG micro-pipe.

2. Model description and governing equations
2.1 Material properties of FGM pipes
The geometrical parameters for FG material micro-pipes are used as those utilized by Deng et al [13] as $D/d = 0.9$, D=20 μm, length l of FGM micro-pipes is assumed 17.6 μm, the density of fluid is $\rho_f = 1000 \ kg/m^3$, as shown in Figure 1. In addition, the mechanical properties for constituent materials are displayed in Table 1.
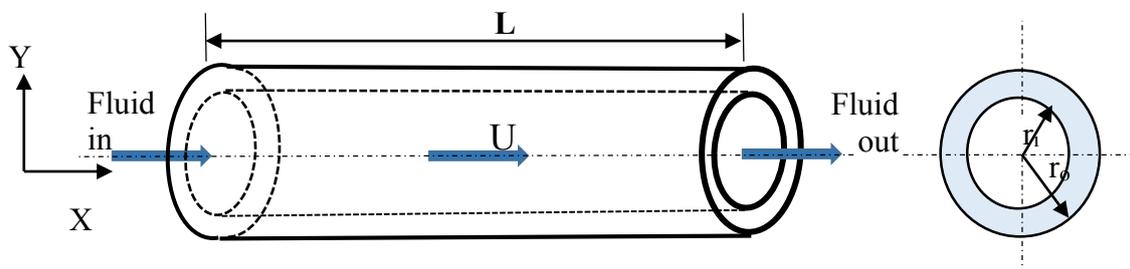

Figure 1. The Geometrical model of a single FGM micro-pipe fluid-conveying.

Table 1. Material properties of FG micro pipe.

Materials	E (Gpa)	ρ_p(kg/m³)	v
Alumina	380	3800	0.23
Aluminum	70	2700	0.23

Most researchers adopted sigmoid law, exponential law, and power law to characterize the material properties variation. A volume fraction of an outer surface constituent of the FGM micro-pipes used in this thesis can be appeared as [14]:

$$v_m = \left(\frac{2z+h}{2h}\right)^n \quad \text{Where} \quad (0 \le n \le \infty) \tag{1}$$

$$v_c = 1 - v_m \tag{2}$$

Where n is the power gradient index, which characterizes the profile of volume fraction during the thickness and is a very positive number; also, subscripts of m and c indicate the metal and ceramic layers, respectively.

It is clear that the material properties vary continuously from alumina-rich at the inner surface for a micro-pipe to aluminum-rich at the outer surface. A change of volume fraction V_m with thickness direction for various values of exponents of volume fraction n is depicted by Figure 2, it can be noted that when the exponent n is supposed to be zero, FGM micro-pipe reduces to homogeneous micro pipe [13].
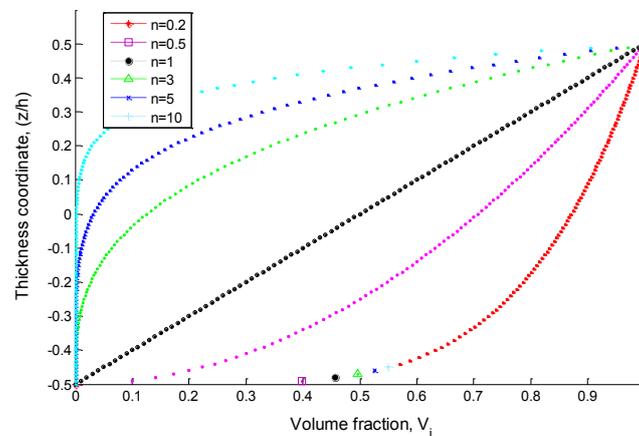

Figure 1. Difference of volume fraction V_m along thickness direction, for many values of a gradient index n.

An effective modulus of elasticity $E(z)$ and the effective density $\rho(z)$ for power-law exponent are given as:

$$\rho(z) = v_m \rho_m + v_c \rho_c \tag{3}$$

$$E(z) = v_m E_m + v_c E_c \tag{4}$$

After substituting Eqs. (1) and (2) into Eqs. (3) and (4), the variation of modulus of elasticity, and density are:

$$E(z) = E_c(E_R - 1)\left(\frac{2z+h}{2h}\right)^n + E_c \tag{5}$$

$$\rho(z) = \rho_c(\rho_R - 1)\left(\frac{2z+h}{2h}\right)^n + \rho_c \tag{6}$$

where $E_R = E_m/E_c$ and $\rho_R = \rho_m/\rho_c$, respectively.

2.2 Mathematical formulation

Based on Euler–Bernoulli beam theory, the offset field for an arbitrary point along the x and z-axes can be written as:

$$\bar{u}(x,z,t) = u(x,t) - Z\frac{\partial w(x,t)}{\partial x} \tag{7}$$

$$\bar{w}(x,z,t) = w(z,t) \tag{8}$$

Where (z) is a coordinate measured from the plane of a neutral axis and t denoted time.
 Assuming that micro-pipe is elastic, the relation of stress–strain is given by:

$$\sigma_{xx} = E\varepsilon_{xx} \tag{9}$$

$$\varepsilon_{xx} = -\frac{\partial w(x,t)}{\partial x} \tag{10}$$

2.3 Modified couple stress theory
The coupled stress theory is a more public form of the theories of higher order continuum, which looks both antisymmetric and uniform parts of higher order deformation gradients. The brief review of this theory was first presented by Xia and Wang and Ahangar et al [15, 16], respectively. The expression of strain energy U refer to the linear elastic material occupying zone Ωi with very small deformation is given by:

$$U_s = \sum_{i}^{s} \frac{1}{2}\int_{\Omega} (\sigma_{ij}\varepsilon_{ij} + \tau_{ij}\gamma_{ij})d\Omega_i \tag{11}$$

$$U = \frac{1}{2}\int\int_{0}^{L} \left[E(z)z^2 + G(z)l^2\right]\left(\frac{\partial^2 w}{\partial x^2}\right)^2 dxdA \tag{12}$$

Or

$$U = \frac{1}{2}\int_{0}^{L} \left(EI_{eq} + GA_{eq}l^2\right)dx \tag{13}$$

Where

$$EI_{eq} = \int_{0}^{2\pi R_m} \int_{-h/2}^{h/2} E(z)z^2 dzdr \tag{14}$$

$$GA_{eq} = \int_{0}^{2\pi R_m} \int_{-h/2}^{h/2} \frac{E(z)}{2(1+v)} dzdr \tag{15}$$

The kinetic energy of FGM micro-pipe and fluid is known as follows [13]:

$$T_p = \frac{1}{2}\rho A_{eq}\left(\frac{\partial w}{\partial t}\right)^2 dx \tag{16}$$

$$T_f = \frac{m_f}{2}\int_{0}^{L}\left[\left(\frac{\partial w}{\partial t} + \alpha u_f\frac{\partial w}{\partial x}\right)^2 + \alpha u_f^2\right]dx \tag{17}$$

The mass of the fluid and pipe per unit length, m_f and m_p respectively. Their expressions can be given as:

$$m_p = \int\limits_{0}^{2\pi R_m} \int\limits_{-h/2}^{h/2} \rho(z)dzdr \;, m_f = \rho_f \rho_f \tag{18}$$

Where ρ_f is the density of fluid in FGM micro-pipe and A_f is the flow cross-sectional area.

2.4 Governing equations

The governing equations for FGM micro-pipe conveying fluid are derived by extended Hamilton's principles as [17]:

$$\delta \int\limits_{t1}^{t2} (T_p + T_f + W_b - U_s)dt = 0 \tag{19}$$

After substitute equations (13), (16) and (17) into equation (19). The equation of motion for FGM micro pipe convening fluid is:

$$\left(EI_{eq} + GA_{eq}l^2\right)\left(\frac{\partial^4 w}{\partial x^4}\right) + \alpha m_f u_f^2 \frac{\partial^2 w}{\partial x^2} + 2m_f u_f \frac{\partial^2 w}{\partial x \partial t} + \left(m_f + m_p\right)\frac{\partial^2 w}{\partial t^2} = 0 \tag{20}$$

Where α is a factor referred to the effect of micro-flow velocity [18]. The non-dimensional form for the equation of motion for FGM micro pipe convening fluid is:

$$(\gamma + \mu)\left(\frac{\partial^4 \eta}{\partial \xi^4}\right) + \alpha u^2 \frac{\partial^2 \eta}{\partial \xi^2} + 2uMr^{0.5}\frac{\partial^2 \eta}{\partial \xi \partial \tau} + \frac{\partial^2 \eta}{\partial \tau^2} = 0 \tag{21}$$

where:

$$\xi = \frac{x}{L}, \quad \eta = \frac{w}{L}, \quad \beta = \frac{m_f}{m_f + m_p}, \quad k_w = \frac{K_w L^4}{E_c I_o}, \quad \gamma = \frac{EI_{eq}}{E_c I_o}, \quad u = \sqrt{\frac{m_f}{E_c I_o}}u_f L$$

$$\mu = \frac{GA_{eq}l^2}{E_c I_o}, \quad \tau = \sqrt{\frac{E_c I_o}{(m_f + m_p)}}\frac{t}{L^2} \tag{22}$$

In this model, three standard BCs of FG micro-pipe are used as shown in Figure 3. And these boundary conditions are written in non-dimensional form as follows:

1- Simply support

$$At \;\; \xi = 0 \rightarrow \eta(\xi) = 0, \;\; \frac{\partial^2 \eta(\xi)}{\partial \xi^2} = 0$$

$$At \;\; \xi = 1 \rightarrow \eta(\xi) = 0, \frac{\partial^2 \eta(\xi)}{\partial \xi^2} = 0 \tag{23}$$

2- Clamped-Clamped

$$At \;\; \xi = 0 \rightarrow \eta(\xi) = 0, \;\; \frac{\partial \eta(\xi)}{\partial \xi} = 0$$

$$At \;\; \xi = 1 \rightarrow \eta(\xi) = 0, \frac{\partial \eta(\xi)}{\partial \xi} = 0 \tag{24}$$

(a)   (b)
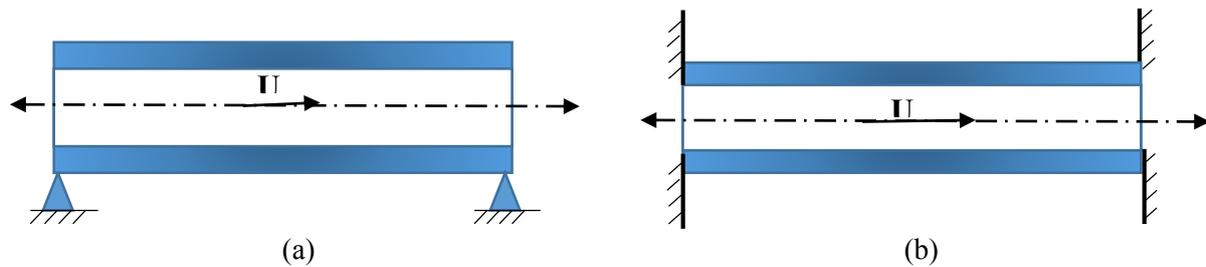
Figure 2. The boundary conditions for FGM micro-pipe for: a) S-S, and b) C-C.

2.5 Galerkin's method

The concept of stability boundary will be extended to use to verify the stability of fluid-conveying micro-pipes as they are gyroscopic systems. Also, in dealing with this method, the Galerkin's scheme is first used to separate the motions equation contained in Eq. (21). By assuming the following series solution [11];

$$\eta(\xi,\tau) = \sum_{r=1}^{\infty} \phi_r(\xi) q_{\eta_r}(\tau) \tag{25}$$

Where, $\phi_r(\xi)$ and $q_{\eta_r}(\tau)$ are the shape functions and the generalized coordinates, respectively. Substituting Eq.(25) into Eq.(21), the following matrix equation can be obtained:

$$\left((\gamma+\mu)[C] + \alpha u^2[A] + 2uMri w[B] - w^2[I]\right)\{q_r\} = 0 \tag{26}$$

where [I]: is identity matrix, and

$$[A]=\begin{bmatrix} \int_0^1 \phi_1''\varphi_1 d\xi & \int_0^1 \phi_2''\varphi_1 d\xi \\ \int_0^1 \phi_1''\varphi_2 d\xi & \int_0^1 \phi_2''\varphi_2 d\xi \end{bmatrix}, [B]=\begin{bmatrix} \int_0^1 \phi_1'\varphi_1 d\xi & \int_0^1 \phi_2'\varphi_1 d\xi \\ \int_0^1 \phi_1'\varphi_2 d\xi & \int_0^1 \phi_2'\varphi_2 d\xi \end{bmatrix}, [C]=\begin{bmatrix} \int_0^1 \phi''''_1\varphi_1 d\xi & \int_0^1 \phi_2''''\varphi_1 d\xi \\ \int_0^1 \phi_1''''\varphi_2 d\xi & \int_0^1 \phi_2''''\varphi_2 d\xi \end{bmatrix} \tag{27}$$

where $\emptyset_1$ and $\emptyset_2$ are the first and second pipe mode functions for a specific end conditions. The analysis for the two conservative FG micro-pipes is given as follows;

A) Simply-Support Micro-Pipe

After substituting the mode functions and the Eigen-values for (S-S) micro-pipe which gave in Tables 2 and 3 into Eq. (27) and implementing the integrations or making utilize of an orthogonal idea, the matrices $[A]$, $[B]$ and $[C]$ can be estimated. Substituting these matrices into Eq. (26) and simplifying gives a single matrix equation. For nontrivial solution one must have:

$$\begin{vmatrix} -0.5w^2 + 7.116\times10^{-14} Mruwi - 4.9348\alpha u^2 + 80.3 & 5.421\times10^{-20} R + 2.667 iwMru \\ 2.168\times10^{-19}\alpha u^2 - 2.67 iwMru & -0.5w^2 + 2..85\times10^{-13} wiMru - 19.739\alpha u^2 + 1284.8 \end{vmatrix} = 0 \tag{28}$$

After solving the determinant in Eq. (28), the following characteristic equation can be obtained:

$$0.25\omega^4 - 1.7791\times10^{-13} i\omega^3 Mru + 12.337\omega^2\alpha u^2 - 7.1108\omega^2 Mr^2 u^2 - 682.58\omega^2$$
$$- 2.8094\times10^{-12} i\omega\alpha Mru^3 + 1.1429\times10^{-10} i\omega Mru + 97.408(\alpha u^2)^2 \tag{29}$$
$$- 7925.6\alpha u^2 + 103188 = 0$$

B) Clamped-Clamped Micro-Pipe

Substituting the mode functions and the Eigen-values for (C-C) micro-pipe which gave in Tables 2 and 3 into Eq. (27) and proceed as for the case of simply supported micro pipe gives the following characteristics equation of the root locus for clamped –clamped pipes as;

$$1.0003\omega^4 - 0.00604i\omega^3 Mru + 58.352\omega^2\alpha u^2 - 44.741\omega^2 Mr^2 u^2 - 7097.5\omega^2$$
$$- 0.16056i\omega\alpha u^3 Mr + 1.1658i\omega Mru + 566.57(\alpha u^2)^2 - 115188\alpha u^2 + 5.1763\times10^6 = 0 \tag{30}$$

Table 2. Modes shapes of the beam for various boundary condition [19].

Boundary condition	Mode shape $\emptyset_r(x)$	σ_r
Simply support	$\sin\beta_r x$	
Clamped-clamped	$\cosh\beta_r x - \cos\beta_r x - \sigma_r(\sinh\beta_r x - \sin\beta_r x)$	$\dfrac{\cos\beta_r L - \cosh\beta_r L}{\sin\beta_r L - \sinh\beta_r L}$

Table 3. The characteristic equations and first three natural frequency for three boundary conditions [19].

Boundary condition	Frequency equation	Value of $a_r = \beta_r L$
Simply support	$\sinh a_r \sin a_r = 0$	$a_1 = \pi$, $a_2 = 2\pi$, $a_3 = 3\pi$
Clamped-clamped	$\cosh a_r \cos a_r = 1$	$a_1 = 4.73004$, $a_2 = 7.8532$ $a_3 = 10.9956$

3. Result and discussion

To investigate the sequence of stability for conservative fluid-conveying FG micro-pipes, the alternative approach (i.e., the concept of stability boundary) can be used. This process provides an easy and effective way to analyze the stability of a wide range of fluid velocities.

In order to get the root position of boundary stability, a typical plot for u^2 verses ω^2 for clamped-clamped FGM micro-pipe conveying fluid at n=1, l=17.6, D=20, D/d=0.9, and α=1 was created in Figure 4. The following principles are followed to check the stability behavior [11]:
1. The FGM micro pipe is stable when all roots place to the right of the line $\omega^2 = 0$.
2. The FGM micro-pipe is unstable if one of the two roots lies in a second quarter.
3. At points of intersection of root place with the line $\omega^2 = 0$, the buckling instability starts.
4. At a maximum point of the root position, the flutter instability initiates.

Now, by reference to Figure 4, the sequence of stability can be observed for the following behavior:
- When u^2 between (0-3), the FGM micro pipe is stable because all ω^2 values are located at the right of line $\omega^2 = 0$.
- At u^2 between (3.079-6.11), the FGM micro pipe is under buckling instability because some values of w^2 located to the left.
- The pipe regains its stability case when u^2 between (6.118 - 6.544).
- Flutter instability occurs for FGM micropipe for $u^2 > 6.544$.
- Points A_S and B_S represented the critical buckling points because they fall on the line $\omega^2 = 0$
- The maximum point (i.e. C_S) represents the critical flutter instability point in the plot.

MATLAB packages are developed to investigate an effect of different parameters on the instability of FGM micro-pipes.

In Figures (5a and b) illustrates the stability boundaries at $Mr = 0.1, 0.3, 0.6$ and 0.9 for simply support and clamped-clamped end conditions. The effect of varying Mr is important on flutter instability as described by these figures, where the maximum points are moved to the right with the increase of the Mr or may disappear as shown in Figure 5a for $Mr = 0.3$. Stability regions (i.e., stable, buckling, and flutter) of the $Mr = 0.3$ differ in comparison to $Mr = 0.9$ as shown in Figure 5. However, the mass ratio has no effect on the buckling instability because the points of buckling (intersection points with the line $\omega^2=0$) are not affected in all cases.

The influence of gradient index on stability region of FGM micro-pipe conveying fluid is explained in Figures 6 a and b. Character (As) represents the stable position, and (Bs) represents the buckling instability, while flutter instability is represents by (Cs) for many values of a gradient index n=1, 3, 10, and 100. It can be seen that a flutter instability and dimensionless natural frequency are increased with an increased in gradient index for simply support and clamped-clamped, respectively.
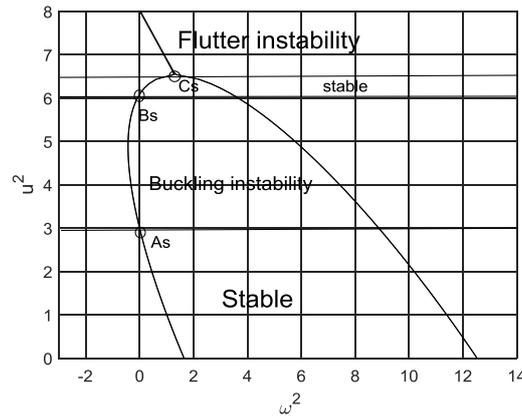
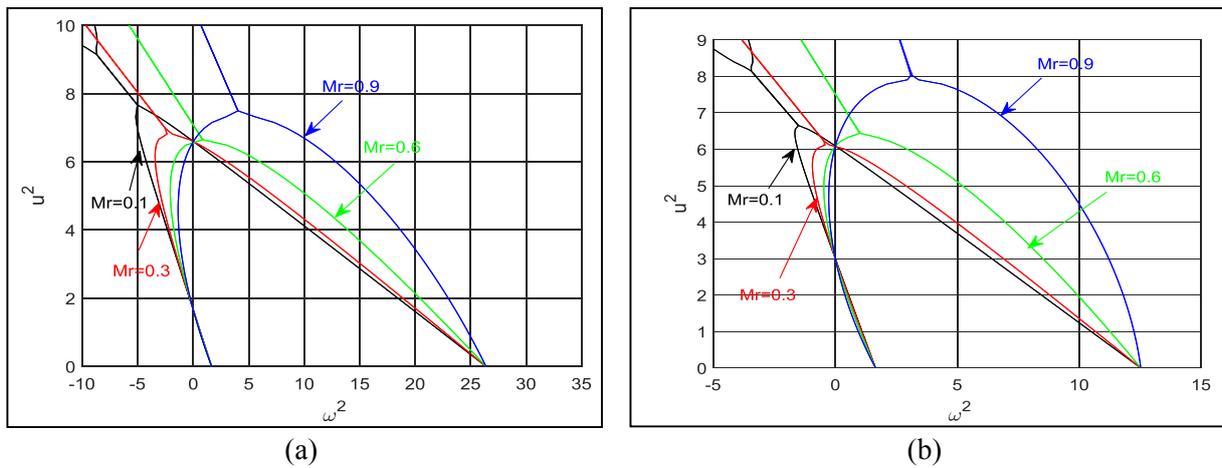Figure 4. Stability boundary for clamped-clamped FGM micro pipe conveying fluid at n=1.

(a)	(b)

Figure 5. Stability boundary of FGM micro-pipe for: (a) S-S (b) C-C.

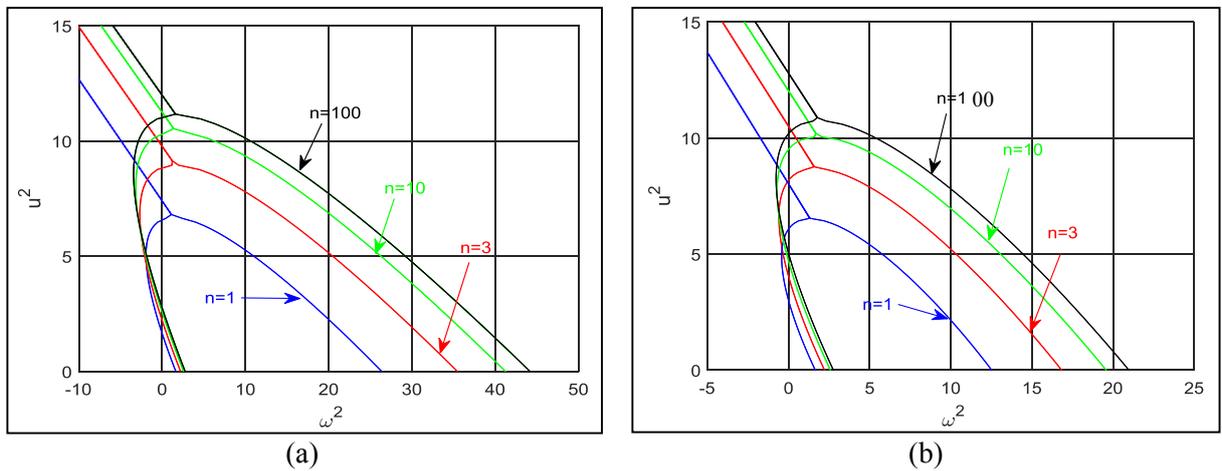
(a)	(b)

Figure 6. Stability boundary of FGM micro-pipe for: (a) S-S (b) C-C.

In Figures (7a, and b) illustrate the influence of micro flow parameter on stability region of FGM micro-pipe conveying for α=1 and 4/3. We noted that the dimensionless natural frequency and the flutter instability are decreased with an increased in micro flow parameter, but the maximum points on a plots are either shifted to right as α increased as in Figure (7a and b) for simply support and clamped-clamped, respectively.

The influence of the length scale on the stability region of FGM micro-pipe conveying is presented in Figures (8a and b) where *l*=15, 17.6, and 20 ʍm are selected. It may be noted that a flutter instability will be increased with the increased in length scale. The effect of increasing n, α and *l* is the slight shift of the

boundary of stability to higher values for all FGM micro-pipes as described in these figures. However, the sequence of stability does not change.

Figure 9 shows a comparison between the homogenous and functionally graded material micro pipe conveying fluid for (S-S and C-C) end condition. It can be noted from this figure that a dimensionless natural frequency and flutter instability for homogenous micro pipe are higher than FGM micro pipe this is because of the inclusion of the material from ceramic to metal.
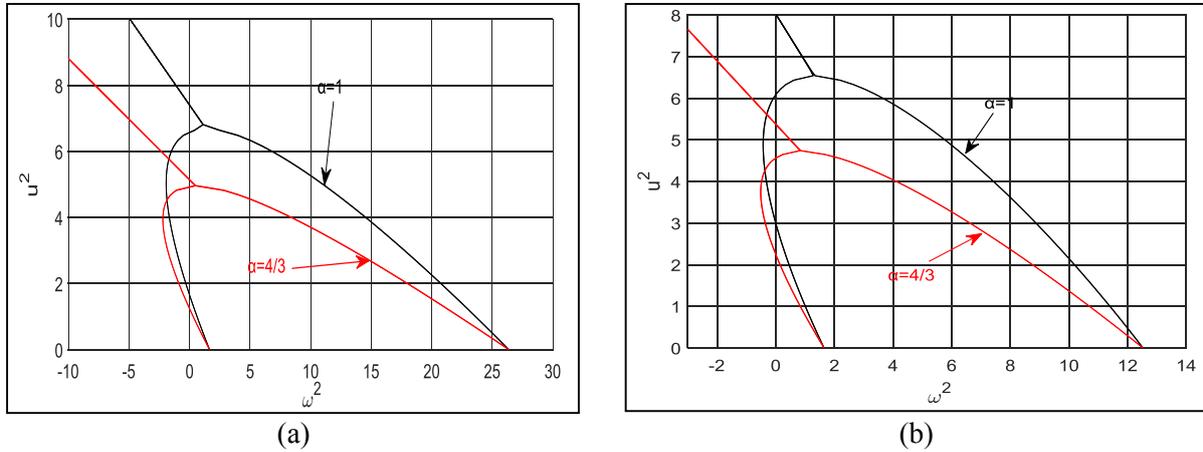

Figure 7. Stability boundary of FGM micro-pipe for various value of micro flow parameter α for: (a) S-S and (b) C-C.
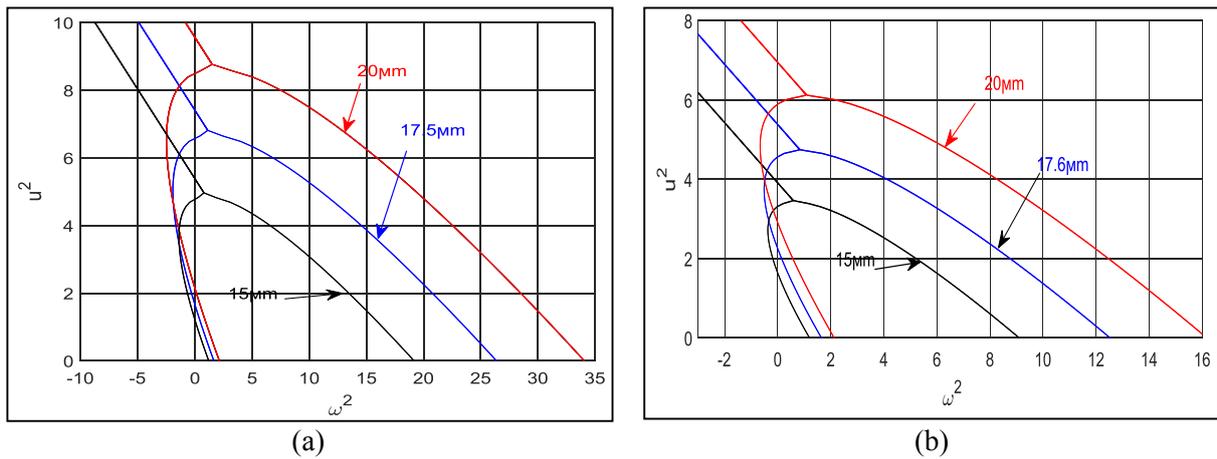

Figure 8. Stability boundary of FGM micro-pipe for varies value of length scale for: (a) S-S and (b) C-C.
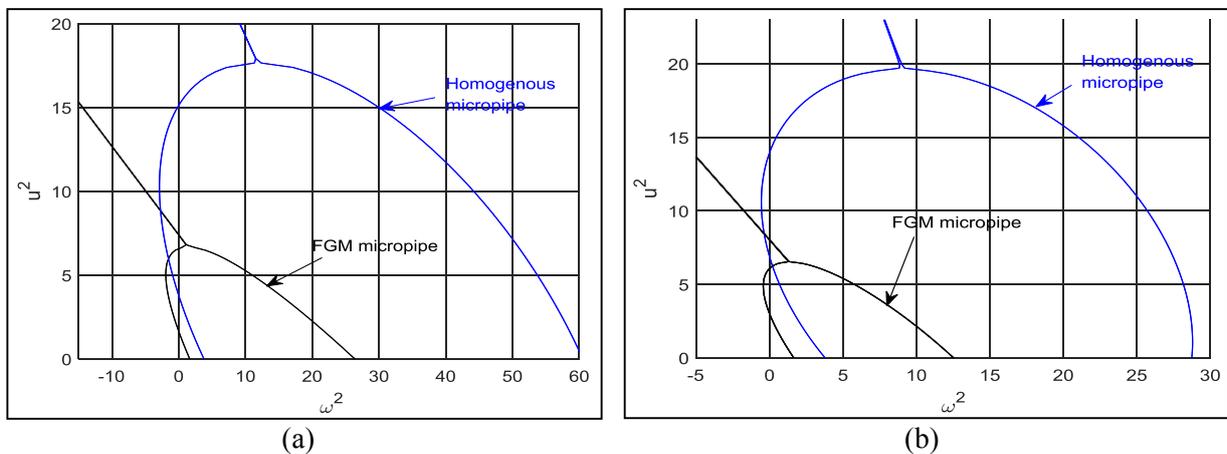

Figure 9. Stability boundary for homogenous micro-pipe and FGM micro-pipe a) S-S and b) C-C end condition.

4. Conclusion

The stability for conservative FG material micro-pipe conveying fluid are investigated in this paper. Equations of motion are acquired by stratifying a modified couple stress (MCS) theory and the Hamilton's principle. Thereafter, the Galerkin's method is progressed to find a complex eigenvalue. Some main inferences acquired from the results above are offered as follows:

1. The fluid -mass ratio has an important influence on a flutter instability and the stability conduct.
2. The increase in a gradient index n and length scale l lead to increase in the flutter instability and dimensionless natural frequency by the amount of increasing 34.2% for S-S and 32.2 % for C-C. It can be modified by the distribution of natural frequencies readily by designing of the gradient index n and length scale l.
3. The dimensionless natural frequency and the flutter instability are decreased with an increased in micro flow parameter by the amount of decreasing 27.1% and 28.7% for S-S and C-C, respectively.
4. The dimensionless natural frequency and flutter instability for homogenous micro pipe are higher than FGM micro pipe by the amount 61.04% for S-S and 67.13% for C-C, this is because of the gradient of the material from ceramic to metal.
5. To test the stability of any conservative FGM micro-pipe, the graphical results presented in this study can be used.

References

[1]   Weaver, D. S., and T. E. Unny. "On the dynamic stability of fluid-conveying pipes." Journal of Applied Mechanics 40, no. 1 (1973): 48-52.
[2]   Bishop, Richard Evelyn Donohue, and I. Fawzy. "Free and forced oscillation of a vertical tube containing a flowing fluid." Philosophical Transactions of the Royal Society of London. Series A, Mathematical and Physical Sciences 284, no. 1316 (1976): 1-47.
[3]   Ryu, Si-Ung, Yoshihiko Sugiyama, and Bong-Jo Ryu. "Eigenvalue branches and modes for flutter of cantilevered pipes conveying fluid." Computers & structures 80, no. 14-15 (2002): 1231-1241.
[4]   Huseyin, K., and R. H. Plaut. "Divergence and flutter boundaries of systems under combined conservative and gyroscopic forces." NASA STI/Recon Technical Report A 76 (1975): 182-205.
[5]   Huseyin, K. "Standard forms of the eigenvalue problems associated with gyroscopic systems." Journal of Sound and Vibration 45, no. 1 (1976): 29-37.
[6]   Kuiper, G. L., and A. V. Metrikine. "On stability of a clamped-pinned pipe conveying fluid." Heron 49, no. 3 (2004): 211-232.
[7]   Chen, Li-Qun, and Wei-Jia Zhao. "A conserved quantity and the stability of axially moving nonlinear beams." Journal of Sound and Vibration 286, no. 3 (2005): 663-668.
[8]   Elfelsoufi, Z., and L. Azrar. "Buckling, flutter and vibration analyses of beams by integral equation formulations." Computers & structures 83, no. 31-32 (2005): 2632-2649.
[9]   Plaut, R. H. "Postbuckling and vibration of end-supported elastica pipes conveying fluid and columns under follower loads." Journal of Sound and Vibration 289, no. 1-2 (2006): 264-277.
[10]   Paı, M. P. "The canonical problem of the fluid-conveying pipe and radiation of the knowledge gained to other dynamics problems across applied mechanics." Journal of Sound and Vibration 310, no. 3 (2008): 462-492.
[11]   Yousif, Albert E., Mohsin J. Jweeg, and Mahmud R. Ismail. "An Alternative Approach for Analyzing Stability of Conservative Pipes Conveying Fluid." Al-Nahrain Journal for Engineering Sciences 17, no. 2 (2014): 165-172.
[12]   Jweeg, J., and J. Ntayeesh. "Determination of critical buckling velocities of pipes conveying fluid rested on different supports conditions." International Journal of Computer Applications134, no. 10 (2016): 34-42.
[13]   Jiaquan Deng, Yongshou Liu and Wei Liu. "Size-dependent vibration analysis of multi-span functionally graded material micropipes conveying fluid using a hybrid method." Microfluidics and Nanofluidics 21, no. 8 (2017): 133.
[14]   Mohammad Hosseini, Abbas Zandi Baghche Maryam and Reza Bahaadini. "Forced vibrations of fluid-conveyed double piezoelectric functionally graded micropipes subjected to moving load." Microfluidics and Nanofluidics 21, no. 8 (2017): 134.

[15] Xia W., and L. Wang. "Microfluid-induced vibration and stability of structures modeled as microscale pipes conveying fluid based on non-classical Timoshenko beam theory." Microfluidics and nanofluidics 9, no. 4-5 (2010): 955-962.

[16] Ahangar Sonia, Ghader Rezazadeh, Rasool Shabani, Goodarz Ahmadi, and Alireza Toloei. "On the stability of a microbeam conveying fluid considering modified couple stress theory." International Journal of Mechanics and Materials in Design 7, no. 4 (2011): 327.

[17] Setoodeh A. R., and S. Afrahim. "Nonlinear dynamic analysis of FG micro-pipes conveying fluid based on strain gradient theory." Composite Structures 116 (2014): 128-135.

[18] L. Wang , H.T. Liu, Q. Ni, and Y. Wu "Flexural vibrations of microscale pipes conveying fluid by considering the size effects of micro-flow and micro-structure." International Journal of Engineering Science 71 (2013): 92-101.

[19] Singiresu S. Rao. "Vibration of continuous systems." John Wiley & Sons Ltd, Hoboken, New Jersey, (2019), 2nd Edition.